


Improved RF Interference Suppression Method

Edward I. Ackerman , *Fellow, IEEE*, and Charles H. Cox III, *Fellow, IEEE*

Abstract—A previously published photonic link architecture was shown to suppress a high-power interference signal of a specific amplitude while permitting recovery of lower-power signals of interest. One undesirable feature of this architecture was the generation of an output intermodulation distortion product that was inherently as strong as the output signal at the frequency of the signal of interest. This article describes a modification to the previously published interference suppression architecture that eliminates this undesirable side effect by applying aspects of one established technique for enhancing the spurious-free dynamic range of analog photonic links along with aspects of a second established technique for accomplishing single-sideband modulation of a Mach–Zehnder electro-optic modulator. The improved performance of this modified architecture is explained using a mathematical model and is verified by the measured input/output characteristics of hardware in a proof-of-concept laboratory demonstration.

Index Terms—Interference suppression, microwave photonics.

I. INTRODUCTION

ANTENNA systems designed to receive signals across a broad range of microwave and/or millimeter-wave frequencies must increasingly contend with a crowded, or even contested, spectral map. This situation motivates development of RF interference suppression techniques to enable the recovery of weak signals of interest while attenuating strong interference signals. The inherently broad bandwidth of photonics technology – especially from a microwave or millimeter-wave frequency standpoint – make it attractive as the basis for a technical approach to enabling RF interference suppression.

A recent paper in this journal [1] surveyed 46 works published since 2003 that describe photonic techniques for RF interference suppression. One such technique suppresses an RF interferer by leveraging the compression characteristic of a photonic link in which modulation of the optical phase and subsequent conversion to intensity modulation is described by cyclic Bessel functions [2]. A low-power signal of interest (SOI) at frequency f_1 plus a higher-power interferer (INT) at frequency f_2 comprised the total input signal to a quadrature-biased Mach–Zehnder (MZ) interferometric modulator supplied with light from a 1,550-nm diode laser, and the output signals from a photodetector connected to the optical output of this modulator were recorded at f_1 and f_2 , at third harmonics $3f_1$ and $3f_2$, and at

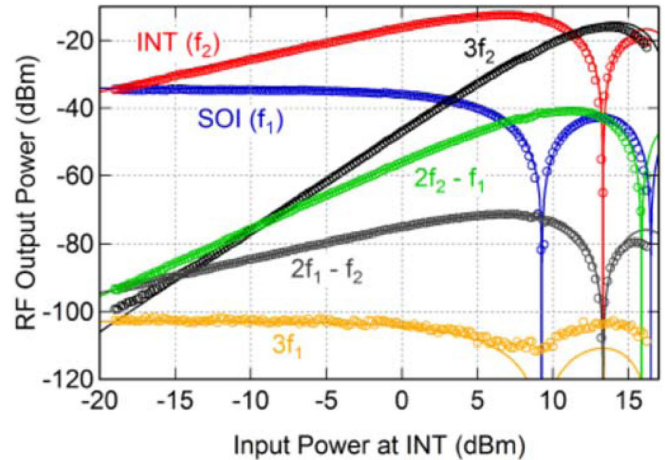


Fig. 1. Output powers from an MZ modulator-based photonic link with an input signal of interest (SOI) at -19 dBm combined with an interferer (INT) at input powers varying from -20 dBm to $+17$ dBm, showing substantial suppression of the interferer (red curve) at the $+13$ dBm input power as reported in [2]. This paper describes a technique for additionally suppressing the problematic intermodulation distortion product (green curve).

problematic third-order intermodulation distortion frequencies $2f_1 - f_2$ and $2f_2 - f_1$. The measured output powers at these frequencies as the input interferer power was varied from -20 dBm to $+17$ dBm are shown in Fig. 1 (from [2]).

The modeled and measured data shown in Fig. 1 confirm the attractive features of the technique described in [2]: its nearly perfect suppression at the interferer input power of approximately $+13$ dBm of both the interferer at frequency f_2 (red curve) and one of the problematic third-order intermodulation distortion frequencies $2f_1 - f_2$ (gray curve) while largely preserving the signal of interest at f_1 (blue curve). Third harmonic frequencies $3f_1$ and $3f_2$ (gold and black curves, respectively) are not minimized at this input power, but usually these can be readily separated from the signal of interest at f_1 . Arguably the least attractive feature of this interference suppression technique is the fact that the second problematic third-order distortion frequency, $2f_2 - f_1$ (green curve in Fig. 1), is not minimized at the input power that suppresses the interferer frequency f_2 . In fact, as shown in Section II of this paper, this distortion product appears at the photodetector with a magnitude exactly equal to that of the signal of interest at f_1 , and is therefore exceedingly difficult to separate from that signal. A second publication using a link architecture similar to the one in [2] reported this same undesirable side-effect [3].

This paper describes a modified photonic link architecture that uses the technique described in [2] and [3] to minimize

Manuscript received February 1, 2020; revised March 17, 2020; accepted April 21, 2020. Date of publication April 30, 2020; date of current version October 1, 2020. (Corresponding author: Edward I. Ackerman.)

The authors are with the Photonic Systems, Inc. Billerica, MA 01281 USA (e-mail: eackerman@photonicsinc.com; ccox@photonicsinc.com).

Color versions of one or more of the figures in this article are available online at <https://ieeexplore.ieee.org>.

Digital Object Identifier 10.1109/JLT.2020.2991633

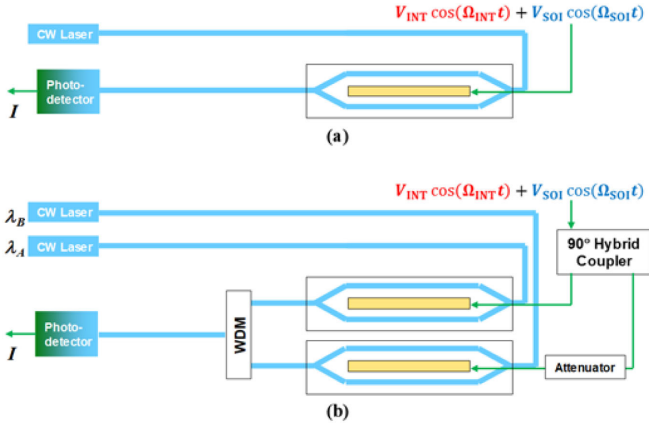


Fig. 2. (a) Mach-Zehnder modulator-based link architecture that suppresses an interferer (INT) while preserving the signal of interest (SOI), but that also generates an intermodulation distortion product equal in magnitude to the SOI [2], [3]; (b) Modified architecture using a wavelength-division multiplexer (WDM) to combine the outputs of two modulators applying the same total input signal to two wavelengths of light at different modulation depths, as guaranteed by the inclusion of an RF attenuator.

the interferer power while largely preserving the power at the signal of interest, and that also minimizes the output power at not just one but both of the problematic third-order intermodulation distortion frequencies.

II. THEORY

The straightforward MZ-modulator based link architecture for which the data in Fig. 1 were measured is shown notionally in Fig. 2(a). The input signal voltage consisting of the strong interferer (INT) and weaker signal of interest (SOI), and the generalized link output current I , are represented using the same notation as in [2]. At the MZ modulator's quadrature bias point, when the input power at the interferer frequency $\Omega_{\text{INT}} = 2\pi f_{\text{INT}}$ is such that $\phi_{\text{INT}} = \pi V_{\text{INT}}/V_{\pi} = 3.8317$ (where V_{π} is the voltage that imposes a π phase difference in the two arms of the MZ),

$$I(f_{\text{INT}}) = 2 I_{dc} J_0(\phi_{\text{SOI}}) J_1(\phi_{\text{INT}}) \cong 0 \quad \text{and} \quad (1)$$

$$I(2f_{\text{SOI}} \pm f_{\text{INT}}) = -2 I_{dc} J_1(\phi_{\text{INT}}) J_2(\phi_{\text{SOI}}) \cong 0 \quad (2)$$

because $J_1(3.8317) \cong 0$. In (1) and (2), I_{dc} is the average photocurrent. These expressions show that the interferer and this third-order intermodulation distortion product are both minimized, whereas the signal of interest is preserved; *i.e.*,

$$I(f_{\text{SOI}}) = 2 I_{dc} J_0(\phi_{\text{INT}}) J_1(\phi_{\text{SOI}}) \cong -0.403 I_{dc} \frac{\pi V_{\text{SOI}}}{V_{\pi}} \quad (3)$$

because $J_0(3.8317) \cong -0.202$. Unfortunately, the other third-order intermodulation distortion product is exactly as strong as $I(f_{\text{SOI}})$ because $J_2(3.8317) \cong 0.202$ and therefore

$$\begin{aligned} I(2f_{\text{INT}} \pm f_{\text{SOI}}) &= -2 I_{dc} J_1(\phi_{\text{SOI}}) J_2(\phi_{\text{INT}}) \\ &= 2 I_{dc} J_0(\phi_{\text{INT}}) J_1(\phi_{\text{SOI}}) \\ &\cong -0.403 I_{dc} \frac{\pi V_{\text{SOI}}}{V_{\pi}}. \end{aligned} \quad (4)$$

The desire to eliminate this side effect of the previously demonstrated ([2], [3]) interference suppression architecture shown in Fig. 2(a) motivated the investigation of potential mitigation approaches.

A. Investigation of Conventional Linearization

When the nonlinearity of one or more components in an RF system results in significantly strong distortion products, as do the interference suppression architectures described in [2] and [3], implementation of a linearization technique can often result in suppression of these undesired distortion products.

In the case of an MZ modulator's distortion products, which are readily predicted because of the modulator's inherently sinusoidal transfer function, many conventional linearization techniques combine the optical outputs of a series or parallel combination of two or more quadrature-biased MZs that are made to modulate a specific ratio of optical carrier powers at a specific ratio of modulation depths such that the third derivative of the overall system's transfer function is minimized [4]–[7]. As with conventional links using a single MZ, quadrature biasing of the multiple MZs in these linearized architectures ensures that all even-order distortion products are also minimized.

For a total input signal $V_{\text{INT}} \cos(\Omega_{\text{INT}} t) + V_{\text{SOI}} \cos(\Omega_{\text{SOI}} t)$ split in a specific voltage ratio r_V and applied to two MZ modulators with the same V_{π} (or split equally and applied to two MZ modulators whose ratio of V_{π} 's is equal to r_V), the components of the output photocurrent I at the two most problematic frequencies f_{INT} and $2f_{\text{INT}} - f_{\text{SOI}}$ are

$$I(f_{\text{INT}}) = 2 I_{dc,A} J_0(\phi_{\text{SOI}}) \left[J_1(\phi_{\text{INT}}) + r_I J_1\left(\frac{\phi_{\text{INT}}}{r_V}\right) \right] \quad (5)$$

and

$$\begin{aligned} I(2f_{\text{INT}} \pm f_{\text{SOI}}) &= -2 I_{dc,A} J_1(\phi_{\text{SOI}}) \left[J_2(\phi_{\text{INT}}) \right. \\ &\quad \left. + r_I J_2\left(\frac{\phi_{\text{INT}}}{r_V}\right) \right], \end{aligned} \quad (6)$$

and the component of the photocurrent at the SOI frequency is

$$I(f_{\text{SOI}}) = 2 I_{dc,A} J_0(\phi_{\text{INT}}) \left[J_1(\phi_{\text{SOI}}) + \frac{r_I}{r_V} J_1\left(\frac{\phi_{\text{SOI}}}{r_V}\right) \right] \quad (7)$$

where $I_{dc,A}$ is the average photocurrent caused by the optical carrier supplied to the modulator for which the input signals impose modulation to a greater depth, and where r_I is the ratio of the photocurrents that would be caused individually by the two optical carriers supplied to the two modulators.

The conventional dual-MZ linearization architecture demonstrated previously in [8] and in many other publications was investigated as a potential means to mitigate the third-order distortion because it was thought that such an architecture would permit equations (5) and (6) to both be made equal to zero non-trivially (*i.e.*, for cases other than $I_{dc,A} = 0$) via prudent control of its three variables: r_V , r_I , and V_{INT} . It was found, however, that a specific property of Bessel functions of the first kind inherently precludes this result. Specifically, at any value of

ϕ for which $J_n(\phi) = 0$, it happens that $J_{n+1}(\phi) = -J_{n-1}(\phi)$. This property inextricably binds the output power of a conventional two-MZ architecture at f_{SOI} to the output power at $2f_{\text{INT}} \pm f_{\text{SOI}}$, just as it did for the single-MZ architecture [as witnessed in equations (3) and (4)].

B. Investigation of the Effect of Adding an RF Phase Shift

To break the bond that ties the magnitudes of the outputs of an MZ-based link at the frequencies f_{SOI} and $2f_{\text{INT}} \pm f_{\text{SOI}}$, the architecture in Fig. 2(b) was investigated. This architecture is the same as the one investigated in Section II.A of this paper, but now with the necessary split of the input RF signal into two paths being accomplished by a 90° hybrid coupler. The outputs of two modulators driven by the same total input signal, but with two optical carriers (at different wavelengths, at least for the case shown) modulated at two different depths, are optically combined (in this case, using a wavelength-division multiplexer) for photodetection using a single device.

Mathematically, the architecture shown in Fig. 2(b) is a promising means of breaking this problematic bond for the same reason that the use of a 90° hybrid coupler to enable application of appropriately phase-shifted RF signals to the two electrodes of a dual-drive modulator successfully breaks the symmetry with which modulation sidebands are imposed on the upper and lower sides of an optical carrier, as has also been demonstrated previously (*e.g.*, [9]). In the case of the link shown in Fig. 2(b), the application of a 90° RF phase shift to the signal applied to one of the two MZ modulators allows for the two components at $2f_{\text{INT}} \pm f_{\text{SOI}}$ from the two modulators to be made equal in amplitude and 180° out of phase with one another while the two components at f_{SOI} are made to be equal in amplitude but only 90° out of phase so that they do not subtract completely at the output of the photodetector.

The expressions for the most relevant spectral components of the output of the photodetector in the link configuration shown in Fig. 2(b) are:

$$I(f_{\text{INT}}) = I_{dc,A} J_0(\phi_{\text{SOI}}) \left[J_1(\phi_{\text{INT}}) + j r_I J_1\left(\frac{\phi_{\text{INT}}}{r_V}\right) \right] \quad (8)$$

$$I(2f_{\text{INT}} \pm f_{\text{SOI}}) = -I_{dc,A} J_1(\phi_{\text{SOI}}) \left[J_2(\phi_{\text{INT}}) + \frac{r_I}{r_V} J_2\left(\frac{\phi_{\text{INT}}}{r_V}\right) \right], \quad (9)$$

and

$$I(f_{\text{SOI}}) = I_{dc,A} J_1(\phi_{\text{SOI}}) \left[J_0(\phi_{\text{INT}}) + j \frac{r_I}{r_V} J_0\left(\frac{\phi_{\text{INT}}}{r_V}\right) \right]. \quad (10)$$

If, as before, ϕ_{INT} remains equal to 3.8317 (the first zero of J_1), if the RF attenuator is set such that $r_V = 3.8317 \div 7.0152$ (the second zero of J_1) = 0.5462, and if the modulators are biased at opposite-slope quadrature points with resulting output powers at an effective ratio $r_I = -0.7331$, then equations (8) and

TABLE I
POSSIBLE COMBINATIONS OF SETTINGS AT THE LOWEST THREE INPUT INTERFERER POWERS (* IN DBM, FOR $V_\pi = 3.75$ V) THAT CAN BE SUPPRESSED BY THE ARCHITECTURE DESCRIBED IN THIS PAPER, THE NECESSARY CORRESPONDING VALUES OF r_V AND r_I , AND THE RESULTING UNDESIRABLE SUPPRESSION (IN DB) OF THE SIGNAL OF INTEREST

Smaller zero of J_1	Larger zero of J_1	Corresponding Interferer Power (dBm)*	r_V	r_I	Suppression of Signal of Interest (dB)
3.8317	7.0152	28.5	0.5462	-0.7331	10.5
	10.1735	31.7	0.3766	+0.6075	12.1
	13.3237	34.3	0.2876	-0.5305	13.2
7.0152	10.1735	31.7	0.6896	-0.8289	12.1
	13.3237	34.3	0.5265	+0.7237	13.2
10.1735	13.3237	34.3	0.7636	-0.8732	13.2

(9) are both approximately equal to zero, whereas

$$I(f_{\text{SOI}}) = -0.4028 I_{dc,A} \frac{\pi V_{\text{SOI}}}{V_\pi} [1 + j], \quad (11)$$

which is only equal to zero when $V_{\text{SOI}} = 0$ or when the optical power supply is removed causing $I_{dc,A} = 0$.

The values of $r_V = 0.5462$ and $r_I = -0.7331$ mentioned above represent just one of many possible solutions when setting the link output signal magnitudes at both f_{INT} and $2f_{\text{INT}} \pm f_{\text{SOI}}$ equal to zero in equations (8) and (9), respectively. Examination of equation (8) shows that two conditions must be satisfied simultaneously to result in zero output signal at f_{INT} : first, the input signal voltage amplitude ϕ_{INT} at f_{INT} must correspond to a zero of the first-order Bessel function J_1 ; second, at this same signal amplitude ϕ_{INT} the value of r_V must cause ϕ_{INT}/r_V to correspond to another zero of the first-order Bessel function J_1 . For any qualifying value of r_V , examination of equation (9) shows that a unique corresponding value of r_I causes the output intermodulation distortion product amplitude at $2f_{\text{INT}} \pm f_{\text{SOI}}$ to equal zero.

Table I lists the lowest three input interferer powers in dBm and corresponding values of r_V that cause equation (8) to equal zero, and the corresponding values of r_I that cause equation (9) also to equal zero. The input interferer powers listed correspond to a modulator with a V_π of 3.75 V, which was the measured V_π of the modulator used in the experiment described in Section III of this paper. If this same modulator had been used in the link described in [2], the interferer power at which suppression occurred would have been equal to 23.2 dBm, or 5.3 dB lower than the interferer input power required by the architecture described in this paper. For $V_\pi = 3.75$ V, the input powers of 23.2 dBm and 28.5 dBm correspond to the two lowest values of $x = \pi \cdot V_{\text{INT}}/V_\pi$ at which $J_1(x) = 0$.

The final column in Table I lists the degree to which the output signal at f_{SOI} is suppressed at the interferer input power that results in complete suppression of the interferer. This undesirable degree of suppression, which was only 7.9 dB for the architecture in [2], is equal to 10.5 dB for the architecture described in this paper, as indicated in Table I. These two values are equal to $-20 \cdot \log[0.4028]$ and $-20 \cdot \log[0.3001]$, where the two quantities in brackets are the magnitudes of the Bessel function J_0 at

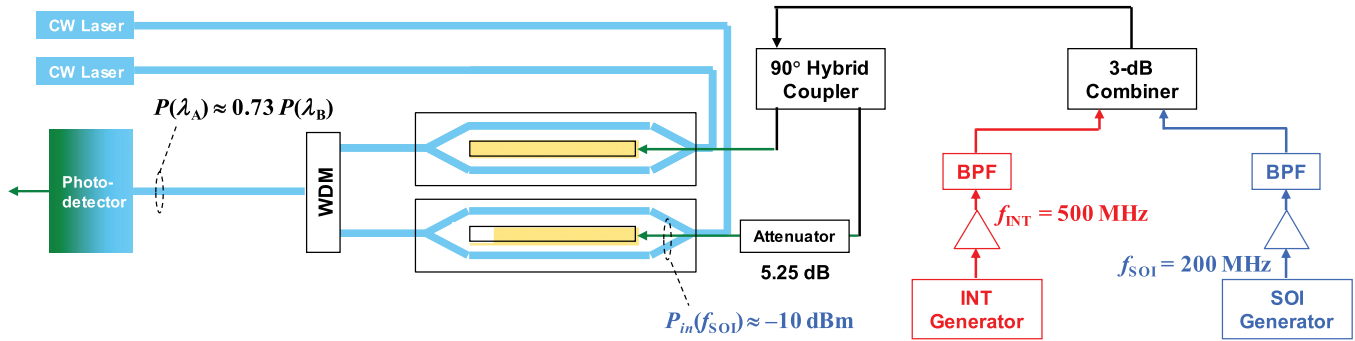


Fig. 3. Experimental set-up for confirmation of the new architecture's effectiveness at suppressing both the interferer at frequency f_{INT} ($= 500$ MHz in this experiment) and at the third-order intermodulation distortion frequency $2f_{INT} - f_{SOI}$ (800 MHz in this experiment) without also suppressing the signal of interest at frequency f_{SOI} (200 MHz in this experiment).

arguments equal to the first and second zeros of J_1 , respectively. The architecture in [2] only required an interferer magnitude that corresponded to the first zero of J_1 . At this first zero of J_1 , J_0 has a larger absolute magnitude than it does at the second zero of J_1 , which is the minimum value to which the input interferer's magnitude must correspond in the architecture described in this paper.

III. EXPERIMENT

An experiment was performed to confirm that the architecture in Fig. 2(b) truly makes it possible to recover a low-power signal of interest while suppressing a stronger interferer without producing a strong 3rd-order intermodulation distortion product – i.e., to confirm the conclusions drawn from the expressions in Section II. A block diagram of the set-up of this experiment is shown in Fig. 3.

As shown in Fig. 3, two signal generators, a 90° RF hybrid coupler, and a 5.25 dB ($= 20 \cdot \log[0.5462]$) RF attenuator were configured in such a way as to apply -10 dBm of power at the signal-of-interest frequency (200 MHz in this experiment) to one modulator and 5.25 dB more than this to the second modulator. The two lasers supplied optical carriers whose powers at the output of the wavelength-division multiplexer were set to a ratio of approximately 0.73:1 when the two modulators were biased at quadrature points on opposite slopes of their transfer functions.

The input power at the interferer frequency (500 MHz in this experiment) was varied from $+7$ to $+23$ dBm in 2 dB steps and in smaller steps thereafter in hopes of not “missing” the one interferer input power at which ϕ_{INT} would yield $J_1(\phi_{INT}) = 0$ for both modulators. For each of these input powers at $f_{INT} = 500$ MHz, the circular markers plotted in Fig. 4 show the measured output powers at $f_{INT} = 500$ MHz and $f_{SOI} = 200$ MHz, at the intermodulation distortion frequencies $2f_{INT} - f_{SOI} = 800$ MHz and $f_{INT} - 2f_{SOI} = 100$ MHz, and at the third harmonic $3f_{INT} = 1.5$ GHz. (The output at the third harmonic of the lower-power signal of interest was too weak to be measured.) The solid-line traces in Fig. 4 show the output powers calculated from equations (8) – (10) and from corresponding expressions for the output power at $f_{INT} - 2f_{SOI}$ and $3f_{INT}$.

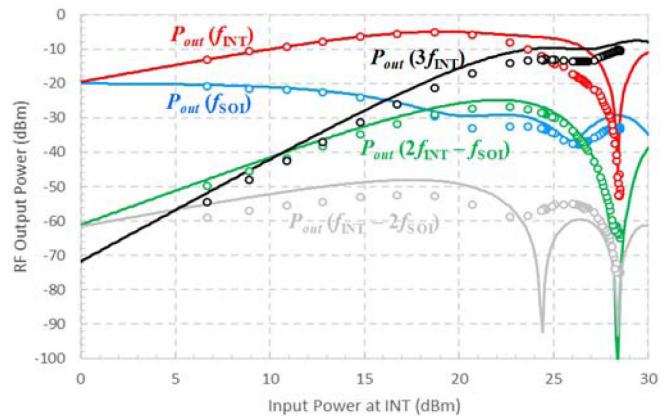


Fig. 4. Plot, for input power of -10 dBm at the signal-of-interest frequency $f_{SOI} = 200$ MHz and for input powers from 0 to $+30$ dBm at the interferer frequency $f_{INT} = 500$ MHz, of the output powers at $f_{INT} = 500$ MHz and $f_{SOI} = 200$ MHz, at the intermodulation distortion frequencies $2f_{INT} - f_{SOI} = 800$ MHz and $f_{INT} - 2f_{SOI} = 100$ MHz, and at the third harmonic $3f_{INT} = 1.5$ GHz as modeled using the expressions in this paper (solid lines) and as measured using the experimental set-up in Fig. 3. At an interferer power of $+28.5$ dBm into the 90° hybrid coupler, the output powers at the interferer frequency and at both third-order intermodulation distortion frequencies are minimized.

The plot in Fig. 4 shows that, at an interferer power of approximately $+28.5$ dBm into the 90° hybrid coupler, the output powers at the interferer frequency and at both 3rd-order intermodulation distortion frequencies are minimized. The output power at the signal-of-interest frequency is partially suppressed at this same input power, though only about as much as it was in the previous interference suppression architecture (see Fig. 1) [2]. Additionally, the 3rd harmonic of the interferer is not minimized (again, as in the original architecture), but this is a far less problematic distortion product.

IV. CONCLUSIONS

With an increasingly congested spectral environment, methods for the suppression of high-power interference signals are presently in high demand. The photonic architecture described in this paper, which improves upon a previously demonstrated

architecture, shows one way that microwave photonics technology can be leveraged to mitigate this situation. It is recommended that future research in this area include repeating the measurements shown in this paper at many more combinations of interferer and signal-of-interest frequencies, and that additional methods for further improving the performance of this architecture be investigated.

ACKNOWLEDGMENT

The authors thank Harold Roussel and Frederick Beihold of Photonic Systems, Inc. for assembling the experiment, and Vincent Urick of DARPA for helpful discussions.

REFERENCES

- [1] V. Urick, M. Godinez, and D. Mikeska, "Photonic assisted interference mitigation," *J. Lightw. Technol.*, vol. 38, no. 6, pp. 1268–1274, Mar. 2020.
- [2] V. Urick, J. Diehl, J. McKinney, J. Singley, and C. Sunderman, "Nonlinear optical angle modulation for suppression of RF interference," *IEEE Trans. Microw. Theory Tech.*, vol. 64, no. 7, pp. 2198–2204, Jul. 2016.
- [3] W. Loh, S. Yegnanarayanan, R. Ram, and P. Juodawlkis, "A nonlinear optoelectronic filter for electronic signal processing," *Sci. Rep.*, vol. 4, Jan. 2014, Art. no. 3613.
- [4] S. Li, X. Zheng, H. Zhang, and B. Zhou, "Highly linear radio-over-fiber system incorporating a single-drive dual-parallel Mach–Zehnder modulator," *IEEE Photon. Technol. Lett.*, vol. 22, no. 24, pp. 1775–1777, Dec. 2010.
- [5] G. Zhu, W. Liu, and H. Fetterman, "A broadband linearized coherent analog fiber-optic link employing dual parallel Mach–Zehnder modulators," *IEEE Photon. Technol. Lett.*, vol. 21, no. 21, pp. 1627–1629, Nov. 2009.
- [6] W. Jiang *et al.*, "A linearization analog photonic link with high third-order intermodulation distortion suppression based on dual-parallel Mach–Zehnder modulator," *IEEE Photon. J.*, vol. 7, no. 3, Jun. 2015, Art. no. 7902208.
- [7] Y. Zhou *et al.*, "Linearity characterization of a dual-parallel silicon Mach–Zehnder modulator," *IEEE Photon. J.*, vol. 8, no. 6, Dec. 2016, Art. no. 7805108.
- [8] E. Ackerman, G. Betts, and C. Cox, "Inherently broadband linearized modulator for high-SFDR, low-NF microwave photonic links," in *Proc. IEEE Int. Topical Meeting Microw. Photon.*, Long Beach, CA, USA, Oct. 2016, pp. 265–268.
- [9] G. Smith, D. Novak, and Z. Ahmed, "Overcoming chromatic-dispersion effects in fiber-wireless systems incorporating external modulators," *IEEE Trans. Microw. Theory Tech.*, vol. 45, no. 8, pp. 1410–1415, Aug. 1997.

Edward I. Ackerman (Fellow, IEEE) received the B.S. degree in electrical engineering from Lafayette College, Easton, PA, in 1987 and the M.S. and Ph.D. degrees in electrical engineering from Drexel University, Philadelphia, PA, in 1989 and 1994, respectively. From 1989 to 1994, he was employed as a Microwave Photonic Engineer by Electronics Laboratory, Martin Marietta, Syracuse, NY. From 1995 to 1999, he was on the research staff at MIT Lincoln Laboratory, Lexington, MA. In 1999, he joined Photonic Systems Inc. Billerica, MA, where he currently is the Vice President of Research and Development. Dr. Ackerman is a Fellow of the IEEE and is currently serving as a Distinguished Microwave Lecturer for the IEEE's Microwave Theory & Techniques Society.

Charles H. Cox, III (Fellow, IEEE) received the B.S.E.E. and M.S.E.E. degrees from the University of Pennsylvania, Philadelphia, PA, in 1970 and 1972, respectively, and the Sc.D. degree from the Massachusetts Institute of Technology (MIT), Cambridge, in 1979. He is currently the President and Chief Executive Officer of Photonic Systems Inc., Billerica, MA, which he founded in 1998 to provide expert consulting services in fiber-optic system design options and to develop low-cost high-performance fiber-optic links for government and commercial applications. Prior to organizing Photonic Systems Inc., he was on the research staff at MIT Lincoln Laboratory, Lexington, MA, as a part of the Applied Physics and Applied Photonics Groups. Dr. Cox is a member of Sigma Xi as well as a Fellow of the IEEE and of the Optical Society of America. He is the author of a textbook, *Analog Optical Links* (Cambridge University Press), 2004.